

## 02 Multitype of cerium centers in optical nanoceramics on the bases of BaF<sub>2</sub>—CeF<sub>3</sub>

© M.Kh. Ashurov<sup>1</sup>, I. Nuritdinov<sup>2</sup>, S.T. Boiboboeva<sup>2,¶</sup>

<sup>1</sup> NPP „Phonon“ of the Republic of Uzbekistan,  
100054 Tashkent, Uzbekistan

<sup>2</sup> Institute of Nuclear Physics, Academy of Sciences of the Republic of Uzbekistan,  
100214 Tashkent, Ulugbek settlement, Uzbekistan

¶e-mail: sohibaboyboboeva@gmail.com

Received May 13, 2022

Revised February 05, 2023

Accepted February 05, 2023

The absorption (SP) and photoluminescence (PL) spectra of BaF<sub>2</sub>—CeF<sub>3</sub> crystals and nanoceramics based on them have been investigated. In samples of both types, under excitation at the excitation band  $\lambda_{\text{ex}} = 285$  nm, a doublet photoluminescence band with maxima at 305 and 320 nm (Ce1 centers) was found. In contrast to this, in optical nanoceramics were found 3 additional PL bands:  $\lambda_{\text{ex}} = 310$  nm,  $\lambda_{\text{rad}} = 370$  nm (Ce2 centers),  $\lambda_{\text{ex}} = 250$  nm,  $\lambda_{\text{rad}} = 425$  nm (Ce3 centers) and  $\lambda_{\text{ex}} = 345$  nm,  $\lambda_{\text{rad}} = 550$  nm (Ce4 centers). The nature of the found centers has been identified.

**Keywords:** fluoride crystals, nanoceramics, absorption spectra, photoluminescence, excitation spectra.

DOI: 10.61011/EOS.2023.03.56181.3678-22

### Introduction

BaF<sub>2</sub> single-crystals offer many excellent physical properties, including non-hygroscopicity, relative ease of machining and polishing, low raw material cost, high melting point (1386 °C) and high thermal conductivity (11.72 W/K at 286 K). These crystals have been widely used as scintillation crystals in  $\gamma$ -radiation detectors because of their high density (4.89 g/sm<sup>3</sup>) and their luminescence at 195 and 220 nm with very short attenuation times of about 800 ps (cross-luminescence band (CL)). Among fluoride compounds, unalloyed BaF<sub>2</sub> crystals are known as the fastest scintillators with a decay time of 0.6 ns and an emission component of 220 nm [1,2]. However, the integral intensity of the fast component is low.

Alongside the above fast components, unalloyed BaF<sub>2</sub> crystals have slow components of auto-localized excitons (ALE) with a maximum at 300 nm and decay time around 700 ns. In many scintillator applications, the relatively slow glow of the ALE is undesirable. The Ce<sup>3+</sup> ion is an active alloying impurity due to the high probability of radiative  $d-f$ -transition [3]. Studies of scintillation properties of BaF<sub>2</sub> doped Ce<sup>3+</sup> crystals with 0 – concentration of 30 mol% showed that with increasing cerium concentration the ALE luminescence disappears [2,4]. The cerium luminescence arising instead of ALE emission has a rather short (20–70 ns) decay time compared to that of ALE luminescence.

Recently, there has been an increasing research interest in optical ceramics (including alkaline earth fluoride crystals) as active laser and scintillation materials [5]. The advantage of ceramics compared to single-crystals is the possibility

of obtaining large aperture samples. The fluoride optical ceramics have been shown to dramatically improve mechanical properties: microhardness increased by 15%, fracture resistance  $K_{1c}$  in 4–6 times [6]. The development of laser fluoride ceramics has been the subject of intensive research in recent years [7–14]. Regarding scintillation ceramics, a significant increase in UV luminescence yield and radiation resistance was recorded for the known scintillator BaF<sub>2</sub>:Ce<sup>3+</sup> [15,16] when transitioning from single-crystals to ceramics [14–16].

In papers [17,18] the structure of CaF<sub>2</sub> and BaF<sub>2</sub> based nanoceramics obtained by hot pressing are investigated. By analyzing electron microscopic photographs of the ceramic chip, the authors identify single-crystalline grains with dimensions on the order of 100  $\mu$ m. A fine lamellar structure is evident within the individual grains. The chip surface is composed of strictly oriented layers with an average width of 30–40 nm for CaF<sub>2</sub>-based<sub>2</sub> nanoceramics and 50–100 nm for BaF<sub>2</sub>-based<sub>2</sub>. Using cross-sectional profiles perpendicular to the direction of the layers, the average layer height was estimated to be 0.5–2 nm for CaF<sub>2</sub>-based nanoceramics and 15 nm for BaF<sub>2</sub>-based.

The difference in microstructure between single-crystals and nanoceramics should lead to the formation of specific types of structural and impurity centers characteristic of nanoceramics. However, the spectral luminescence properties of BaF<sub>2</sub>-based nanoceramic samples have not been investigated in sufficient detail. On this basis, comparative studies of luminescence characteristics of BaF<sub>2</sub>:Ce single-crystals and optical nanoceramics based on them have been carried out in the present paper to reveal specific features of the spectral characteristics.

## Research samples and methodology

BaF<sub>2</sub> crystals doped with 0.12 mol% CeF<sub>3</sub> were grown by vertical directional crystallization [19]. Lead fluoride was used as a fluorinating agent. The ceramics were obtained by hot-pressing [9,10] from powdered precursor prepared according to the method described in papers [20,21]. The base of the precursor is barium hydrofluoride BaF<sub>2</sub>HF, which releases fluorinating agent HF during heat treatment. Cerium fluoride dissolves in the matrix during the sintering process [22]. This process makes it possible to produce ceramics with a 100% density.

The optical transparency of ceramics is determined by the feedstock quality. In contrast to glass welding and single-crystal growth from melt, the technological process of optical ceramics production does not contain the operation of purification of the initial material. Organic impurities and mechanical inclusions of foreign particles in the sample increase light absorption and light scattering. Even a seemingly flawless charge can produce almost opaque ceramics. Increasing the vacuum level leads to improved optical transparency [9,10,20,21].

Optical treatment of the sample surfaces was carried out (Fig. 1).

The optical absorption spectra of the samples were measured with a Specord M-40 spectrophotometer. The PL spectra were measured at room temperature with a setup based on the KSVU-12 and SPM-20 monochromators and excited by a xenon lamp. The excitation part contained a KSVU-12 monochromator, while the registration part — a SPM-20 monochromator and a PMT-106 photomultiplier tube. The resulting spectra are not corrected for PMT sensitivity.

## Experimental results and their discussion

Absorption spectra of unirradiated BaF<sub>2</sub>–CeF<sub>3</sub> crystals show intensive absorption bands with maxima at 205, 285 nm, which are responsible for *f*–*d*-ion transitions Ce<sup>3+</sup> (Fig. 2, curve 1). In addition to these bands, the absorption spectra of the unirradiated ceramic samples show additional bands in the 282 nm area and a weak broad band in the 250 nm area (Fig. 2, curve 2) [16].

Under excitation in the 285 nm band of unirradiated BaF<sub>2</sub>:Ce<sup>3+</sup> crystal, bands with maxima at 305 and 320 nm

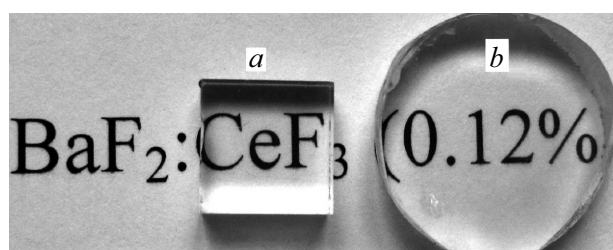


**Figure 1.** Appearance of the single-crystal (a) and ceramic (b) BaF<sub>2</sub>:Ce<sup>3+</sup> samples examined.

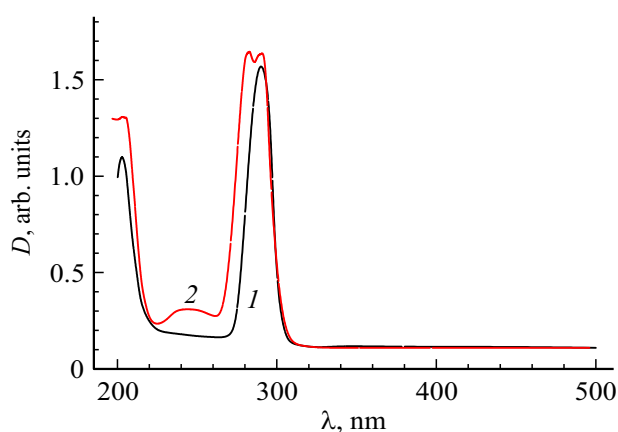


**Figure 2.** Absorption spectra of unirradiated samples of single-crystals (1) and nanoceramics (2) based on BaF<sub>2</sub>:CeF<sub>3</sub>.

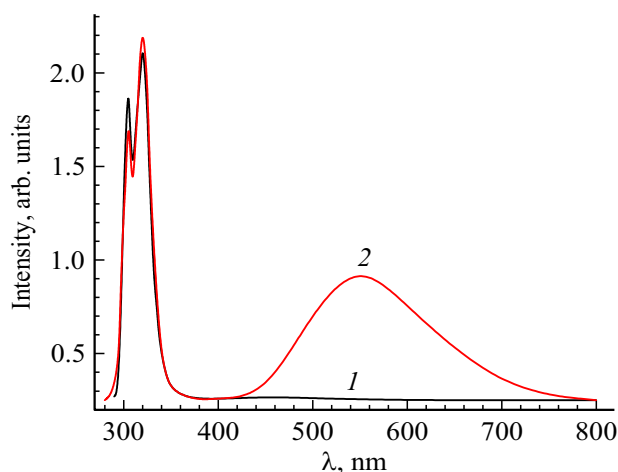


**Figure 3.** PL spectra at excitation in the 285 nm band of unirradiated BaF<sub>2</sub>:Ce<sub>3</sub> (1) and unirradiated ceramics (2).

are observed in the PL spectrum (Fig. 3, curve 1). In the 200–800 nm spectral area of the unirradiated crystal BaF<sub>2</sub>:Ce<sup>3+</sup>, no other PL bands are detected.

In PL spectra of unirradiated BaF<sub>2</sub>:Ce<sup>3+</sup> ceramics under excitation in 285 nm band, besides 305 and 320 nm luminescence bands available in single-crystals, additional broad band with maximum in 550 nm area was found (Fig. 3, curve 2). It should be noted that, as in the paper [5], in the ceramic samples compared to crystals, the intensity of the PL band at 305 nm is enhanced relative to the band at 320 nm.

Excitation spectra of 305 and 320 nm PL bands are identical in unirradiated crystalline and nanoceramic BaF<sub>2</sub>:Ce<sup>3+</sup> samples, there are bands with maximum at 285 nm (Fig. 4, curves 1, 2). In the excitation spectrum of the 550 nm PL band of the BaF<sub>2</sub>:Ce<sup>3+</sup> ceramic sample, bands with maximums at 250, 285 and 345 nm are observed (Fig. 4, curve 3). The 285 nm band — is the excitation band of the 305 and 320 nm maximum PL bands as it strongly overlaps with the 250 and 345 nm excitation bands.

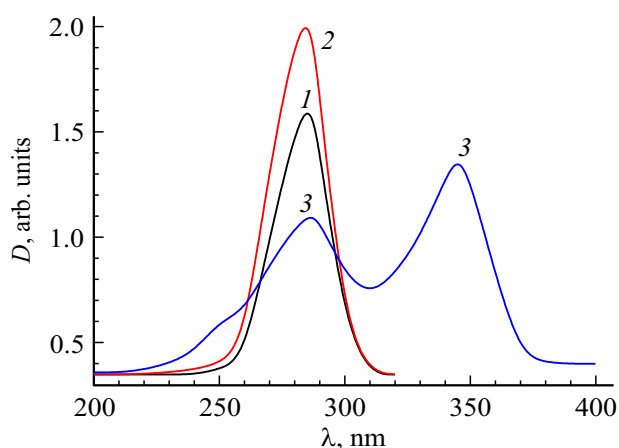


**Figure 4.** Excitation spectra of  $\text{BaF}_2:\text{Ce}^{3+}$  ceramics in luminescence bands 305 (1), 320 (2) and 550 nm (3).

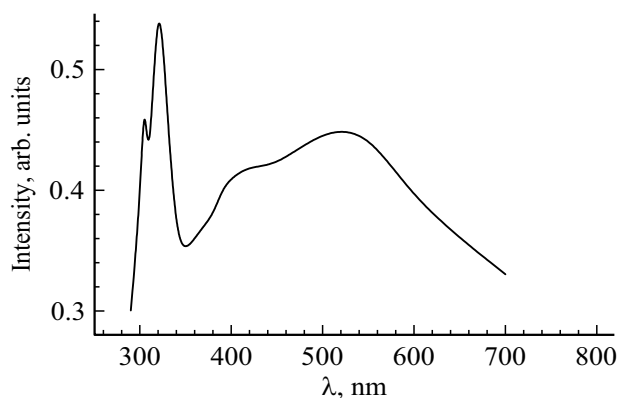


**Figure 5.** The PL spectrum of unirradiated  $\text{BaF}_2:\text{Ce}^{3+}$  ceramics under excitation at the tail of the 250 nm (240 nm) band.

Under excitation on tail of the 250 nm band (i.e., at  $\lambda_{\text{ex}} = 240$  nm) of unirradiated  $\text{BaF}_2:\text{Ce}^{3+}$  ceramics, PL bands with maximums at 305, 320, 380, 425 and 550 nm are found (Fig. 5). The contributions of the 305 and 320 nm bands to the luminescence are greatly reduced with excitation in the 250 and 345 nm bands compared to the excitation in the 285 nm band as it is due to the excitation of the 305 and 320 nm PL bands on the tail of the 285 nm excitation band. This is because the 285 nm excitation band strongly overlaps with the tails of the 250 and 345 nm excitation bands. On the other hand, in the excitation spectrum of the 550 nm PL band the intensity of the 250 nm excitation band has the lowest intensity. Therefore the 250 nm absorption band cannot be the 550 nm luminescence band since the most intense excitation band of this PL band is at 345 nm. We consider the 345 nm band to be the PL excitation band at 550 nm. The occurrence of the 550 nm PL band upon excitation in the 285 nm band is due to the 320 nm luminescence reabsorption since this PL band strongly overlaps with the 345 nm excitation band. With this in mind, we identify

the 250 nm excitation band as the PL excitation band at 425 nm.

The complexity of the absorption and PL spectra of ceramic samples as compared to single-crystals can be attributed to the presence of cerium ions in defective positions, namely localized at grain boundaries or dislocations [23].

The emission of cerium ions in area  $\lambda = 280 - 360$  nm is due to electronic transitions  $5d-4f$  in the  $\text{Ce}^{3+}$  ions. The luminescence intensity under X-ray excitation depends on the cerium concentration and reaches a maximum value at a concentration of 0.1 mol%. A further increase in the cerium concentration leads to a decrease in the luminescence intensity. Concentration quenching of X-ray cerium luminescence may be due to either an increase in the probability of emission-free transitions in excited cerium ions or a decrease in the probability of cerium ion excitation in the electron-hole recombination process [3].

We have not been able to reliably determine the 380 nm excitation band of the PL. However, given that in the paper [3] found a luminescence band with a maximum of 370 nm, which is excited in the 310 nm band, we can conclude that the 380 nm luminescence band we found is the 370 nm band found in [3]. Therefore, we believe that the 380 nm band is excited in the 310 nm band.

Considering that

1) Ce1-centers are found in both  $\text{BaF}_2-\text{CeF}_3$  based single-crystals and nanoceramics;

2) In single-crystals at the investigated cerium concentration no luminescence of other cerium centers was detected besides Ce1-centers;

3) According to the work of [24], in single-crystals  $\text{BaF}_2-\text{CeF}_3$  at concentrations  $\text{CeF}_3$  of 0.1 mol%, single trigonal cerium centers are mostly formed, Ce1 centers are identified as trigonal cerium  $\text{C}_{3V}$ -centers.

With increasing impurity concentration, paired and more complex impurity centers, including various clusters [25], begin to appear in the structure of alkaline earth fluoride crystals. Based on this fact and also taking into account the opinion of the authors of [3], we attribute Ce2 centers to paired cerium centers whose luminescence is caused by  $5d-4f$  — transitions in  $\text{Ce}^{3+}$  ions, shifted towards lower energies due to interaction with other neighboring  $\text{Ce}^{3+}$  ions.

In paper [5] the luminescence of cerium ions was detected in  $\text{BaF}_2:\text{CeF}_3$  based optical ceramics in the 300 to 450 nm wavelength range. The authors suggested that this long wavelength wing of luminescence is due to optical centers perturbed compared to isolated centers due to changes in the local impurity environment associated with the presence of various defects or impurities in the cerium environment. The latter may be due to the fact that the synthesis of ceramic samples in their structure forms single-crystalline grains of the order of  $100 \mu\text{m}$ , between which a thin layered structure of nanometric size [17,18] is formed. The regular crystalline structure is disrupted at the boundaries of the single-crystalline grains and between

the nanolayers. Cerium dissolves in the matrix during the sintering process [22]. This leads to the formation of new defect states around cerium impurities located at the boundaries of grains and nanolayers, which lead to additional absorption and PL bands of impurity centers in the spectrum compared to single-crystals.

In paper [26], a study of pulsed cathodoluminescence of  $\text{CeF}_3$  crystals has revealed a low-intensity narrow luminescence band with a maximum at 543 nm, which the authors attribute to inter-combination transitions between singlet and triplet transitions within an isolated divalent ceria center  $\text{Ce}^{2+}$  formed in the electron irradiation process. The authors [26] assume that the  $\text{Ce}^{3+}$  ion in the ground state is ionized directly or through the  $6s$  state by electron radiation, transforming into the  $\text{Ce}^{4+}$  ion. An electron is knocked out of the conduction band from an  $\text{Ce}^{3+}$  ion and captured by another  $\text{Ce}^{3+}$  ion, forming an  $\text{Ce}^{2+}$  ion in an excited state from which it can have emission transition to the ground state  $^3H_4$  emitting a broad luminescence band with peaks at 433 and 487 nm or nonradiatively to the  $^1D_2$  level. Further, there is a emission transition from the  $^1D_2$  level of ion  $\text{Ce}^{2+}$  to  $^3H_4$  level, which corresponds to a narrow band with a wavelength of 543 nm.

Since the single-crystalline samples were produced by melting (by vertical directional crystallization) and the nanoceramic samples were synthesized without melting (by hot pressing from powdered precursor, where dissolution of cerium fluoride in matrix occurs in the sintering process), in the nanoceramics some of the cerium fluoride may not have completely dissolved in barium fluoride and be the source of 550 nm luminescence.

A comparative analysis of our results and the literature shows the following.

1. If the nature of the band with maximum 550 nm we found would be due to inter-combination transitions of the divalent cerium center, then this band should appear in both single-crystalline and nanoceramic samples since it corresponds to transitions of the isolated cerium center and cerium ions in both single-crystals and nanoceramics are preferably in isolated state. However, the luminescence band with maximum at  $\lambda \sim 550$  nm was detected by us only in ceramic samples.

2. As the authors of [26] themselves state, it is difficult to realize excitation to the level  $^1D_2$  of the divalent cerium ion in the PL study. However, in our studies the PL band is easily excited in the 345 nm band.

3. The luminescence, due to inter-combination transitions on divalent cerium centers, is narrow [26], but the luminescence we detected is broadband.

Taken together the above facts show that the 550 nm band is not related to inter-combination transitions in the non-dissolved barium fluoride phase of  $\text{CeF}_3$ , but conditioned on the creation of complex defect states at grain boundaries and interlayer boundaries.

## Conclusion

Thus, in single-crystalline samples of  $\text{BaF}_2:\text{CeF}_3$ , trigonal cerium  $C_{3V}$ -centers (denoted as Ce1-centers) are mainly formed which give rise to luminescence bands with 305 and 320 nm maxima ( $\lambda_{\text{ex}} = 285$  nm). The presence of intergranular and interlayer boundary transition areas in nanoceramics leads to the formation of additional impurity cerium centers relative to single-crystals. As a result, new bands with maxima 282 and 250 nm are formed in absorption spectra of nanoceramics and in PL spectra, except for  $C_{3V}$ -centers observed in single-crystalline samples, appear additional bands with 370 maximums ( $\lambda_{\text{ex}} = 310$  nm) caused by Xe2-centers, 425 maximums ( $\lambda_{\text{ex}} = 250$  nm) — Xe3-centers, and 550 maximums ( $\lambda_{\text{ex}} = 345$  nm) — Xe4-centers. Nature of the detected new cerium centers in nanoceramic samples: Ce2-centers are identified as paired cerium centers, Ce3- and Ce4-centers — cerium centers in complex with different defective states at grain boundary interfaces and interlayer interfaces in nanoceramics.

## Acknowledgments

The authors are deeply grateful to P.P. Fedorov for kindly providing samples for the study of  $\text{BaF}_2:\text{CeF}_3$  single-crystals and nanoceramics based on them.

## Funding

The paper was prepared on a fundamental research theme № PP-4526 of the Institute of Nuclear Physics of the Academy of Sciences of the Republic of Uzbekistan.

## Conflict of interest

The authors declare that they have no conflict of interest.

## References

- [1] G. Benemanskaya, E. Garibin, Yu. Gusev, A. Demidenko, S. Ivanov, V. Ivochkin, S. Kosianenko, I. Mironov, Yu. Mousienko, V. Jmerik, V. Reiterov, D. Seliverstov, T. Shubina. *J. Nuclear. Instruments and Methods in Physics Research A*, **610** (1), 335 (2009).
- [2] R. Visser, P. Dorenbos, C.W.E. van Eijk, R.W. Hollander. *J. IEEE. Transactions on Nuclear Science*, **38** (2), 178 (1991).
- [3] R. Visser, P. Dorenbos, C.W.E. van Eijk, A. Meijerink, G. Blase, H.W. den Hartog. *J. Phys.: Condens. Mater.*, **5**, 1659 (1993).
- [4] P. Dorenbos, R. Visser, C.W.E. van Eijk, R.W. Hollander, H.W. den Hartog. *J. Nucl. Instrum. Methods A*, **310**, 236 (1991).
- [5] P.P. Fedorov, V.V. Osiko, T.T. Basiev, Y.V. Orlovsky, K.V. Dukelsky, I.A. Mironov, V.A. Demidenko, A.N. Smirnov. *Rossiyskiye nanotekhnologii*, **2** (5), 95 (2007) (in Russian).
- [6] M.Sh. Akchurin, R.V. Gaynutdinov, P.L. Smoliansky, P.P. Fedorov. *Dokl. RAN*, **406** (2), 180 (2006). (in Russian).

- [7] S.H. Bagytov, L.S. Bolyasnikova, E.A. Garibin, V.A. Demidenko, M.E. Doroshenko, K.V. Dukelsky, A.A. Luginina, I.A. Mironov, V.V. Osiko, P.P. Fedorov. Dokl. Akademii nauk, **422** (2), 179 (2008). (in Russian).
- [8] T.T. Basiev, M.E. Doroshenko, P.P. Fedorov, V.A. Konyushkin, S.V. Kuznetsov, V.V. Osiko, M.Sh. Akchurin. Opt. Lett., **33** (5), 521 (2008).
- [9] M.Sh. Akchurin, T.T. Basiev, A.A. Demidenko, M.E. Doroshenko, P.P. Fedorov, E.A. Garibin, P.E. Gusev, S.V. Kuznetsov, M.A. Krutov, I.A. Mironov, V.V. Osiko, P.A. Popov. Opt. Mater., **35** (3), 444 (2013).
- [10] P.P. Fedorov. *Fluoride laser ceramics*, ed. by B. Denker, E. Shklovsky (Woodhead, Oxford, 2013), p. 82.
- [11] M.E. Doroshenko, A.A. Demidenko, P.P. Fedorov, E.A. Garibin, P.E. Gusev, H. Jelinkova, V.A. Konyushkin, M.A. Krutov, S.V. Kuznetsov, V.V. Osiko, P.A. Popov, J. Shulc. Phys. Status Solidi C, **10** (6), 952 (2013).
- [12] A. Lyberis, A. Stevenson, A. Suganuma, S. Ricaud, F. Druon, F. Herbst, D. Vivien, P. Gredin, M. Mortier. Opt. Mater., **34**, 965 (2012).
- [13] S.V. Kuznetsov, A.A. Alexandrov, P.P. Fedorov. Inorg. mater., **57** (6), 583 (2021). (in Russian).
- [14] P.A. Rodny, S.D. Gain, I.A. Mironov, E.A. Garibin, A.A. Demidenko, D.M. Seliverstov, Y.I. Gusev, P.P. Fedorov, S.V. Kuznetsov. FTT, **52** (9), 1780 (2010). (in Russian).
- [15] A.A. Demidenko, E.A. Garibin, S.D. Gain, Yu.I. Gusev, P.P. Fedorov, I.A. Mironov, S.B. Michrin, V.V. Osiko, P.A. Rodnyi, D.M. Seliverstov, A.D. Smirnov. Opt. Mater., **32** (10), 1291 (2010).
- [16] P.P. Fedorov, M.H. Ashurov, Sh.G. Boboyarova, S.T. Boyboyoyeva, I. Nuritdinov, E.A. Garibin, S.V. Kuznetsov, A.N. Smirnov. Neogranicheskiye mater., **52** (2), 1 (2016). (in Russian)
- [17] P.A. Popov, K.V. Dukelsky, I.A. Mironov, A.N. Smirnov, P.L. Smoliansky, P.P. Fedorov, V.V. Osiko, T.T. Basiev. DAN **412** (2), 185 (2007). (in Russian)
- [18] M.Sh. Akchurin, R.V. Gaynutdinov, E.A. Garibin, Y.I. Golovin, A.A. Demidenko, K.V. Dukelsky, S.V. I.I. Golovin, A.A. Demidenko, K. Dukelsky, S. Kuznetsov, I.A. Mironov, V.V. Osiko, A.N. Smirnov, N.Y. Tabachkova, A.I. Turin, P.P. Fedorov, V.V. Shindyapin. Perspektivnye materialy, **5**, 5 (2010) (in Russian).
- [19] P.P. Fedorov, V.V. Osiko. In: *Bulk Crystal Growth of Electronic, Optical and Optoelectronic Materials*, ed. by P. Capper. Wiley Series in Materials for Electronic and Optoelectronic Applications (John Wiley & Son, Ltd. 2005), p. 339–356.
- [20] A.A. Luginina, P.P. Fedorov, A.E. Baranchikov, V.V. Osiko, E.A. Garibin. Patent RU 2545304 daed 24.02.2015, priority of 27.06.2013.
- [21] A.A. Luginina, A.E. Baranchikov, A.I. Popov, P.P. Fedorov. Mater. Res. Bull., **49** (1), 199 (2014).
- [22] S.Kh. Batygov, M.N. Mayakova, S.V. Kuznetsov, P.P. Fedorov. Nanosystems, **5** (6), 752 (2014).
- [23] P.P. Fedorov, S.V. Kuznetsov, A.N. Smirnov, E.A. Garibin, P.E. Gusev, M.A. Krutov, K.A. Chernenko, V.M. Khanin. Neogranicheskiye mater., **50** (7), 794 (2014). (in Russian)
- [24] S.A. Kazansky, A.I. Ryskin. FTT, **44** (8), 1356 (2002). (in Russian).
- [25] T.T. Basiev. AFRL-AFOSR-UK-TR-2013-0063. EOARD CRDF 06-9001 / CRDF RUP2-1517-MO-06
- [26] O.A. Snigireva, V.I. Solomonov. FTT, **47** (8), 1392 (2005). (in Russian).

Translated by Y.Deineka